Canrea Journal: Food Technology, Nutritions, and Culinary, 2024; 7 (2): 162–179 OPEN ACCESS

e-ISSN : 2621-9468

Canrea Journal: Food Technology, Nutritions, and Culinary is licensed under a Creative Commons Attribution 4.0 International License, which permits unrestricted use, distribution, and reproduction in any medium, provided the original work is properly cited.

Type of the Paper (Article)

Characterization of resistant starch (type III) produced from banana (*Musa acuminata* x *balbisiana* CV Awak) pseudostem

Lee-Hoon Ho[1*], Rashneve Segar[1], Fairus Shalini Mathihalagan[1], Siti Husna Zakaria[2], and Sharifah Amirah Husna Tuan Mazlam[2]

[1] School of Food Industry, Faculty of Bioresources and Food Industry, Universiti Sultan Zainal Abidin, Besut Campus, 22200 Besut, Terengganu, Malaysia
[2] Centralized Lab Management Centre, Universiti Sultan Zainal Abidin, Besut Campus, 22200 Besut, Terengganu, Malaysia

Abstract

Banana (*Musa acuminata* x *balbisiana* cv. Awak) is rich in macro- and micro nutrients. The global surge in banana production has led to significant waste, with 60% of the biomass including banana pseudostem, being discarded. This contributes to environmental issues and has prompted research into converting this waste into valuable products. It is rational to process banana pseudostem into useful products, such as functional food ingredients. This study aimed to produce type III resistant starch from banana pseudostem, focusing on analyzing its functional properties and examining the morphology of the produced resistant starch. Emphasizing type III resistant starch derived from the underutilized agricultural byproduct, banana pseudostem, presents a novel approach to developing functional food ingredients. The native starch from banana pseudostem was isolated and processed into resistant starch (type III) through an autoclaving process. The characterization of resistant starch from banana pseudostem (RSBP) was compared with native banana starch and commercial starch (i.e., corn and potato) in terms of functional groups, crystalline structure, paste clarity, pH, freeze thaw stability, particle size distribution, and morphology. The results showed that hydroxy, alkene, carbonyl, and alkane groups were present in all the evaluated starches, but the sulphate group was found only in RSBP. Moreover, RSBP exhibited a B-type crystalline structure. The native starch from banana pseudostem had a smooth surface devoid of dents, with a mixture of irregularly shaped granules, including oval, spheroid, and elongated forms. All evaluated starches were categorized as acidic food ingredients. Potato starch had the highest paste clarity (91.17%) and particle size distribution (45.22μm). RSBP exhibited significantly higher freeze thaw stability than the other starches. Banana pseudostem can be considered a feasible low-cost raw material for producing type III resistant starch, allowing for the, development of suitable functional foods, depending on the desired end-product quality.

Article History
Received August 23, 2023
Accepted October 6, 2024
Published December 31, 2024

Keywords
Banana Pseudostem, Resistant Starch, Functional Properties, Starch Morphology.

1. Introduction

Banana plants, members of the *Musaceae* family, are native to the Malaysia-Indonesian region of South-East Asia (1). Bananas provide important nutrients for health, including resistant starch, total dietary fibers, rapidly and slowly digestible starches, and potassium, a

* Correspondence : **Lee-Hoon Ho** holeehoon@unisza.edu.my/ holeehoon@yahoo.com

ISSN 2621-9468 online, DOI 10.20956/canrea.v7i2.1109

major supplier of macro-elements. Bananas are the fourth most important food product worldwide, after rice, wheat, and corn, especially in developing countries (2). In Malaysia, bananas are the second most widely cultivated fruit, with banana plantations covering an area of about 23,000 hectares and a total production of 0.3 million metric tons in 2022 (3). According to Silva et al. (4), approximately 40% of banana plants are left as waste in the plantation after harvesting, and about 60-80 tons per hectare of banana pseudostem are generated annually. This underutilized banana pseudostem has the potential to be transformed into value-added, low-cost food ingredients for human consumption.

Starch is one of the most important glycemic carbohydrates found in cereals, roots, tubers, and unripe fruits, contributing up to 70–80% of total carbohydrates in human diets (5). Starch is a polysaccharide made up of two polymers which are amylose, a linear molecule, and amylopectin, a branching molecule (6). According to Luo et al. (7), amylose content is positively correlated with resistant starch. Resistant starch refers to the sum of starch and its degraded products that resist digestion in the small intestine of healthy individuals (8-10). According to Apriyanto et al. (11), starch plays a pivotal role in the food industry due to its unique physicochemical properties. Resistant starch behaves similarly to fiber, as it cannot be digested or absorbed by amylase in the small intestine but can be fermented by colonic microflora in the large intestine (12-14). This fermentation process lowers colonic pH and produces short-chain fatty acids (SCFAs), which promote the growth of beneficial bacteria (15-16). Due to resistant starch's resistance to human digestive enzymes, it is digested slowly, leading to a gradual release of glucose and contributing to a low glycemic index (17). This property can improve glucose regulation in individuals with diabetes and aid in weight management by lowering glycemic and insulinemic responses to food (18-21). Apart from that, resistant starch has been reported to have potential as a unique ingredient that can yield high-quality foods. For example, research shows that products made with resistant starch exhibit improved crispness, expansion, color, mouthfeel, and flavor compared to those produced with traditional, insoluble fibers (22). Resistant starch can be incorporated into a wide range of mainstream food products, such as baked goods, without affecting the processing characteristics or sensory attributes, such as overall appearance and taste (23).

Food grains (i.e., maize, wheat, and sorghum), tubers and roots (i.e., potato and sweet potato), as well as sago, are the raw materials commonly used for the processing resistant starch. However, in Malaysia, the availability of these materials for resistant starch production is limited because the country does not produce wheat and only produces small quantities of corn, rice, and potatoes, which do not meet its needs. Therefore, an alternative source of starch is urgently needed for resistant starch production. According to Subagyo and Chafidz (1), the banana pseudostem contains a high amount of starch that can be utilized as cattle feed. In India, the pith, or tender core, of the banana pseudostem has been used as food after boiling and the addition of spices (24). To our knowledge, there is no published reports on type III resistant starch produced from banana pseudostem. To meet the growing demand, an alternative starch source, such as banana pseudostem, could be utilized in the food industry. For this, understanding the functional properties of type III resistant starch produced from banana pseudostem is a prerequisite. However, knowledge in these areas is lacking, particularly in comparison to commercial starches. Hence, the present study aimed to determine the functional properties of resistant starch (type III) produced from banana pseudostem, as well as to observe its morphology. Furthermore, the characteristics of the produced type III resistant starch were compared to commonly used commercial starches

(corn starch and potato starch) to determine the potential of starch isolated from banana pseudostem as a new ingredient in food preparation.

2. Materials and Methods

2.1. Materials

Matured banana (*Musa acuminata* X *balbisiana* cv. Awak) pseudostem was collected from a banana plantation in Pulau Berangan, Besut, Terengganu, Malaysia. Banana trees with pseudostem diameters ranging from 13 to 15 cm and approximately 10 to 12 months of age were selected for starch production. Commercial corn starch (Cap Bintang, Selangor, Malaysia) and potato starch (Bestari, Selangor, Malaysia) were purchased from Giant Superstore Jerteh, Terengganu, Malaysia. All chemicals used in this study were of analytical grade.

2.2. Isolation of Banana Pseudostem Starch

The native starch from the banana pseudostem was isolated using a simple steeping method, modified from studies by Nakthong et al. (25) and Rahma et al. (26). Prior to isolation, impurities and dirt were removed, and the pseudostems were cleaned and cut into longitudinal pieces before mechanically pressed with excess water. The pressed stems were soaked in distilled water at sample-to-water weight (w/v) ratio of 1:2 for 24 h at 4°C and then filtered using four layers muslin cloth, along with the juice extracted from the banana pseudostem (BP), and left for another 24 h to form crude starch sediment. The resultant starch was collected and washed several times with distilled water to separate the starch fraction with other water-soluble materials. The starch precipitate was dried in a cabinet dryer at 40°C for 8 h and subsequently ground in a laboratory mill before being sieved using a 100-mesh screen. The isolated native BP starch was stored in an airtight bottle for further use.

2.3. Preparation of Resistant Starch (Type III)

Type III resistant starch was produced from native banana pseudostem starch (BPNS) following a method adapted from Zi-Ni et al. (27), with modifications to the isolation conditions, including factors such as starch concentration, enzyme pullulanase concentration, and the number of thermal cycles. In addition, a preliminary study on the optimum condition (i.e., starch concentration (4 %), enzyme pullulanase concentration (40 %), the number of thermal cycle (3 cycle), and a drying temperature (40°C) for producing type III resistant starch from BPNS was conducted using the one-factor-at-a-time method (unpublished data). Native starch (4% weight-per-volume on a dry basis) was suspended in sodium acetate buffer (0.1 M, pH 5) (Sigma-Aldrich, St. Louis, USA). The mixture was autoclaved (Tuttnauer, Hauppauge, USA) at 121°C for 1 h and cooled to 60°C before enzymatic debranching. Pullulanase (Novozymes, Bagsværd, Denmark) (40%) was added to the mixture to debranch the starch. The sample was heated at 80°C for 15 min to inactivate the enzyme. Then, autoclaved at 121°C for 30 min to completely gelatinise the starch.

The sample underwent three temperature cycles to create and develop high-melting type III resistant starch crystals. In the first cycle, the sample was autoclaved at 121°C for 1.5 h to accelerate the type III resistant starch crystal formation, then incubated in a water bath (Thermo Fisher Scientific, Waltham, USA) at 70°C for 3 h to cool the gelatinised starch. In the second cycle, the sample was autoclaved again at 121°C for 1.5 h and then incubated at 70°C

in a water bath for 18 h to initiate crystals growth. In the third cycle, the sample was autoclaved once more again at 121°C for 1.5 h and incubated in a water bath at 70°C for 3 h. After cooling, the sample was oven-dried at 40°C until a constant moisture content was achieved. The sample was ground using a laboratory mill, then sieved using a mechanical sieve shaker to obtain a fine powder (250 mm). All samples were stored in an airtight container before further analysis.

2.4. Determination of Functional Group

Attenuated total reflectance-Fourier transform infrared (ATR-FTIR) spectroscopy (Thermo Fisher Scientific, Waltham, USA) was employed to identify the chemical functional groups present in starch samples. The spectra were obtained using an ATR-FTIR Spectrophotometer (ATRFTIR Shimadzu, Kyoto, Japan) equipped with a DTGS KBr detector and a Golden Gate Single Reflection Diamond ATR accessory at a 45° incident angle. A small amount of starch was applied to cover ATR diamond plate, and the pressure clump was swung down and screwed between the opposing base and tip untill the sample was firmly held in place. Prior to scanning the sample, a background spectrum was collected to account for noise and interference from the instrument and environment. Spectra were recorded in the mid-infrared region (4000–400 cm^{-1}) using 16 scans at a resolution of 4 cm^{-1}. The sample spectrum was corrected by subtracting the background spectrum for clearer identification of functional groups. After measurement, the sample was removed, and the plate was cleaned with a non-abrasive tissue (28).

2.5. Determination of Crystalline Structure

The crystallinity of the samples was analyzed using X-ray diffractometer (Rigaku miniflex (II), Wilmington, USA) operated at a scanning rate of 2.00°/ min. X-ray diffraction patterns were recorded at diffraction angles ranging from 2θ=10°to 80°at room temperature (29). The x-ray diffractogram was generated using Microsoft® Excel® 2019 MSO (version 2301 Build 16.0.16026.20002).

2.6. Observation of Granule Morphology

The morphology of the starch granules was observed using a Field Emission Scanning Electron Microscope (Thermo Scientific™ Quattro Emission Scanning Electron Microscope, Waltham, MA, USA). Samples were mounted on aluminium stubs and coated with platinum in a vacuum atmosphere using Ion Sputter Coater G20 (GSEM, Gyeonggi-do, Republic of Korea) to enhance the conductivity and prevent electrical discharge during scanning. Images were taken at an operating voltage of 5 to 10 kV with magnification from 150x to 1000x (30).

2.7. Determination of Paste Clarity

Paste clarity was measured following the method outlined by Das and Sit (31). A suspension was prepared by adding 0.2 g of the sample to 20 mL of distilled water, which was then heated in a water bath at 90°C for 1 h. After heating, the suspension was cooled to room temperature before measurement. Clarity was assessed by determining the transmittance at 640 nm using UV-VIS spectrophotometer (Thermo Fisher Scientific, Genesys 20, Mississauga, Canada).

2.8. Measurement of pH

Two grams of each sample was weighed and mixed with 50 mL of distilled water, then stirred for 10 min. The mixture was filtered, and the pH of the filtrate was measured using a calibrated pH meter, previously calibrated with pH 7 and pH 4 buffers (32).

2.9. Determination of Freeze Thaw Stability

A starch suspension (5% w/v dry basis) was prepared by dispersing starch in distilled water and heating it for 30 min at 95°C with constant stirring. Ten grams of the resulting paste were transferred into centrifuged tubes and frozen at -20°C for 22 h. After freezing, the paste was thawed for 2 h at 30°C. This freeze- thaw cycle was repeated three times, with samples centrifuged (Eppendorf, Hamburg, Germany) for 10 min at 5000 × g at 20°C after each cycle (33)

Syneresis (%) = Volume of water released / Initial volume of paste x 100

Freeze thaw Stability (%) = 100% - Syneresis

2.10. Determination of Particle Size Distribution

Particle size distribution of starch was determined using a Litesizer particle size analyzer (Litesizer model 500, Anton Paar, Graz, Austria). Approximately 0.25 g of powder was dispersed in 1 mL of water with magnetic agitation. Particle size distribution and the mean particle diameter (d_{50}) were measured for the various starches (34)

2.11. Statistical Analysis

Data from this study were analysed using the Statistical Package for Social Science (SPSS) Statistic version 20.0. All measurements were performed in triplicates (n=3) to obtain mean values. A one-way analysis variance (ANOVA), followed by Duncan's test, was conducted to determine significant differences among mean values of samples at $p<0.05$.

3. Results and Discussion

3.1. Functional Group

Figure 1 depicts the infrared spectra of starches. All the examined samples exhibited peaks in the range of 3500 to 3000 cm^{-1} indicating the presence of hydroxyl groups (35). The presence of hydroxyl groups in starch contributes to its functional properties, such as thickening, gelling, and binding (36). These hydroxyl groups facilitate hydrogen bonding with water, enabling the swelling and breakdown of the granules (37). The peaks at 1000 cm^{-1} and 650 cm^{-1} correspond to stretching vibrations of C=C bond in alkene group (38). There were also peaks associated with the functional group of alkenes. The presence of alkene groups affects the water absorption and swelling behavior of modified starch, making it less soluble in water. This functional group can enhance film-forming ability, adhesion, and binding properties, which can be beneficial in various applications such as food, pharmaceuticals, and paper industries (39).

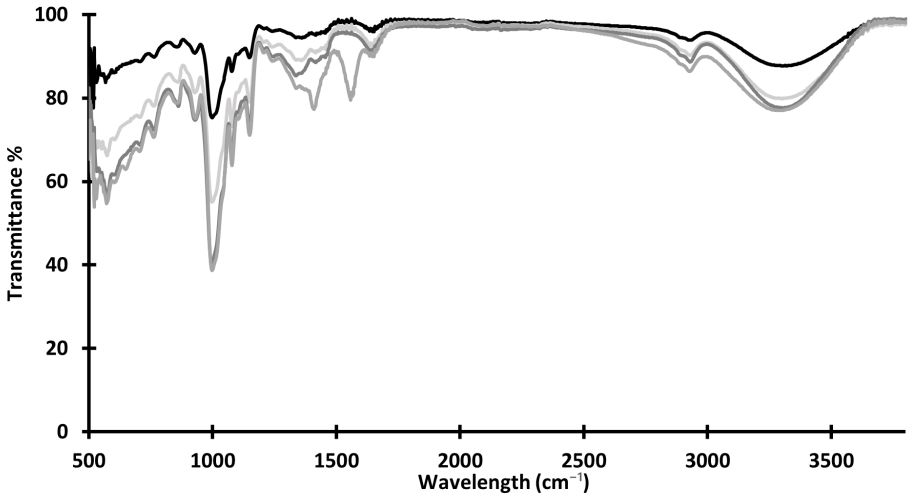

Figure 1. Fourier-transform infrared spectroscopy spectra characters of the starches. ( ): CS (corn starch), ( ): PS (potato starch), ( ): NSBP (native starch of banana pseudostem), ( ): RSBP (resistant starch (type III) of banana pseudostem).

In addition, it was observed that there was spectra at frequencies of 1415–1380 cm^{-1} in the RSBP sample, indicating the presence of sulphate groups. This band confirms that the existence of sulphate has resulted in the RBS being more resistant to enzymatic breakdown by digestive enzymes in the small intestine. This suggests that the starch is less likely to be rapidly digested and absorbed, providing a slower release of glucose into the bloodstream. The peak in the range of 1600 cm^{-1} to 1500 cm^{-1} reflects the presence of weak alkane groups in starch, which increases the hydrophobic nature of the starch, making the material less soluble in water (40). Furthermore, the peak in the range of 1750 cm^{-1} to 1650 cm^{-1} indicates the presence of carbonyl groups in starch (41). These carbonyl groups contribute to the starch's ability to undergo gelatinization, the process of swelling and dissolution of starch granules when heated in water (41). The narrow peak between 3000 cm^{-1} to 2840 cm^{-1} may be attributed to C-H stretching vibration associated with alkane groups (42). Alkane groups can influence the rheological behaviors of starch pastes or solutions, affecting parameters such as viscosity and shear thinning properties (40). Both corn and potato starches display significant absorption around 1000 cm^{-1} due to their polysaccharide nature; however, subtle differences in their molecular structures (such as the ratio of amylose to amylopectin) result in varied functional properties. This impacts their applications in food technology, where understanding these differences is essential for achieving desired textures and thickening qualities. The modification of starches through functional groups such as hydroxyl, carboxyl, and ester groups significantly improve their properties, including solubility, thermal stability, and binding capacity. These enhancements allow for novel applications in areas like biodegradable materials, drug delivery systems, and food processing. For instance, phosphorylated starches provide better freeze-thaw stability in frozen foods, while esterified starches are used in creating biodegradable plastics (43).

Additionally, the intensity of functional groups in starches significantly impacts their rheological properties. For instance, starches with higher degrees of phosphorylation exhibit increased viscosity and enhanced thermal stability compared to those with lower

phosphorylation levels, resulting in more stable pastes under varying temperatures (44). Similarly, the intensity of carboxyl groups affects gel strength and viscosity; starches with higher carboxyl content tend to form weaker gels and exhibit lower viscosities due to disruption of molecular structure (45). These variations in functional group intensity thus lead to distinct rheological behaviors, influencing the suitability of starches for specific applications.

3.2. Crystalline Structure

The X-ray diffraction patterns of native starch of banana pseudostem (NSBP), resistant starch (type III) of banana pseudostem (RSBP), potato starch (PS), and corn starch (CS) are shown in Figure 2. The 2θ value denotes the angle formed between the incident X-ray beam and the diffracted X-ray beam. The intensity of the peaks in the diffractogram corresponds to the amount of X-ray scattering occurring at a particular angle. It is influenced by factors such as the number of scattering centers (atoms or molecules) in the crystal, their arrangement, and the X- ray absorption properties of the material (46). The A-type crystalline structure is typical of cereal starches such as corn, rice, and wheat. The dense arrangement of the A-type crystal structure helps prevent acid hydrolysis of the materials (47). In contrast, the B-type crystalline structure is commonly found in the starches of tubers, fruits, and stems such as banana, potato, canna, and sago (47). The XRD pattern of CS contains diffraction peaks at (2θ) = 15.32°, 17.26°, 18.14°, and 23.26°, which correspond to the A-type crystalline structure. The XRD pattern of PS contains diffraction peaks at (2θ) = 17.34°, 22.50°, and 24.34°, corresponding to the B-type crystalline structure.

Moreover, the diffraction peaks of NSBP (2θ = 15.22°, 17.3°, and 24.04°) and RSBP (2θ = 17.36°, 22.46° and 24.6°) both correspond to the B-type crystalline structure. Furthermore, it was observed that there were four main peaks in corn starch. This may be due to the compact arrangement of granules, which results in high peak intensity. PS and NSBP showed similar patterns in their diffractogram, indicating that they have a similar arrangement of crystalline structure. However, RSBP exhibited lower peak intensity, even though the peaks appeared similar to those of PS and NSBP. This can be explained by the fact that the arrangement of RSBP is more chaotic or random, leading to lower peak intensity (48).

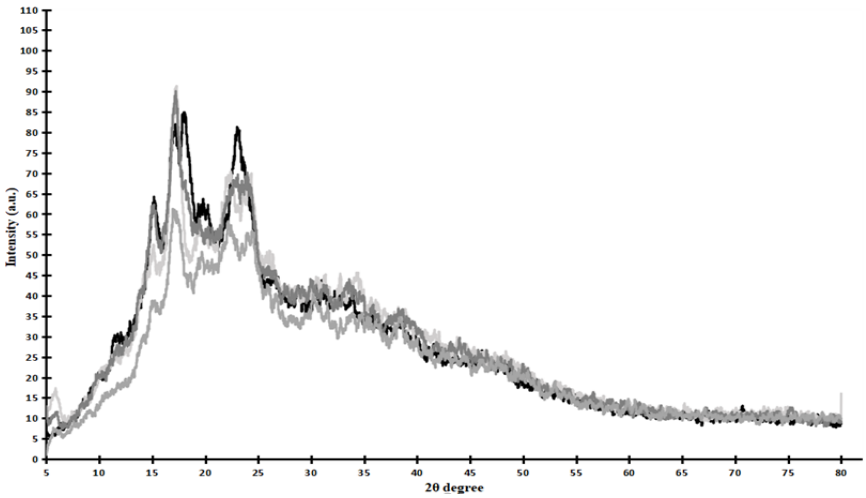

Figure 2. X-ray diffractogram of starches. (—): CS (corn starch), (—): PS (potato starch), (—): NSBP (native starch of banana pseudostem), (—): RSBP (resistant starch (type III) of banana pseudostem).

3.3. Morphology of Granules

The images captured through scanning electron microscopy (SEM) of the samples are shown in Figure 3. Different starch sources and processing methods can result in variations in granule size and shape, which in turn impact the properties of the starch. The morphology of starch granules affects characteristics such as gelatinization, pasting behaviour, and viscosity. Based on the SEM observations, the size of starch granules varied as follows: NSBP (6.5–50.7 µm), RSBP (7.04–125.7 µm), PS (9.7–93.3 µm), and CS (4.35–21.0 µm). According to Utrilla-Coello et al. (49), the granule size for typical starches ranges from 1.0 to about 200.0 µm. The NSBP granules were observed to had irregular, elongated, and round/spheroidal shapes. The morphology of starch isolated form the pseudostem of banana was found to be similar to that of starch isolated from the fruit of banana, as described by Marta et al. (50). The surface of banana starch granules is generally smooth, but it may exhibit irregularities of an oval shape (50). Moreover, the size of banana starch granules can vary depending on the banana variety and ripeness, with ripe bananas usually have larger starch granules compared to unripe ones. The size range contributes to the unique morphology of banana starch (50).

The average granule size of RSBP is larger than that of the other evaluated starches. Moreover, RSBP exhibited surface destruction of the granules, which was due to the autoclaving process involved in the preparation of resistant starch (type III) from native starch. Espinosa-Solis et al. (36) stated that the autoclave treatment led to the gelatinization and disruption of the native structural arrangement of the starch granules.

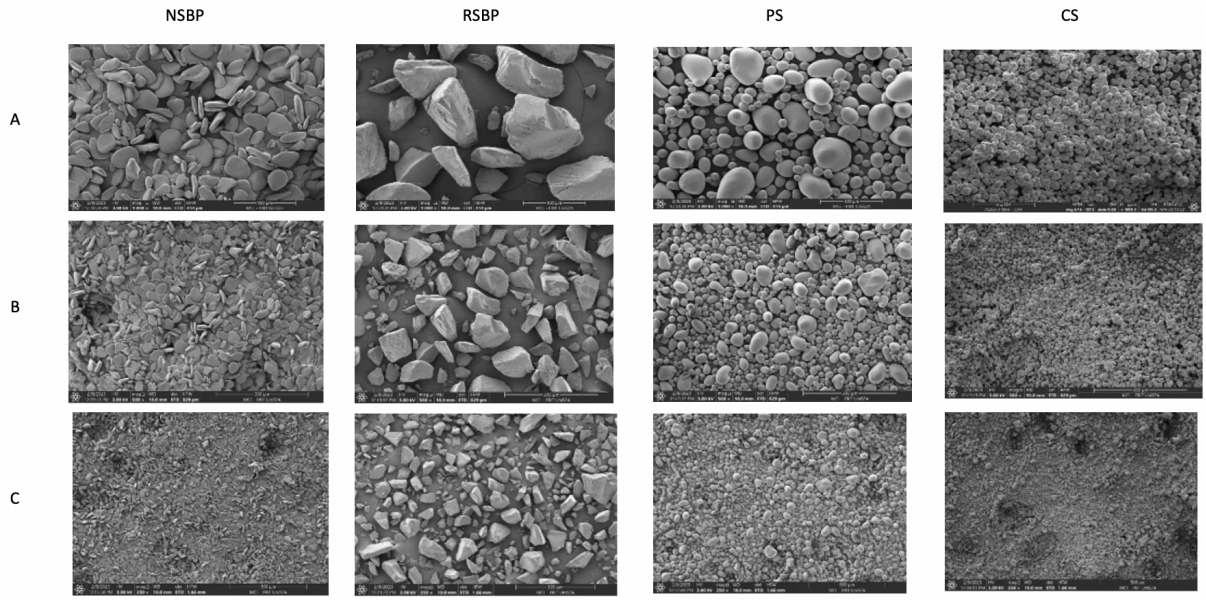

Figure 3. Micrographs of starches. The starches were analyzed at 1000× magnification (A), 500× magnifications (B), and 250× magnifications (C). NSBP: native starch of banana pseudostem, RSBP: resistant starch (type III) of banana pseudostem, PS: potato starch, CS: corn starch.

The CS exhibited granules with the characteristic morphology of regular corn starches, including spherical, elliptical, and polyhedral shapes, as well as granule fragments. The morphology of PS includes oval, round, and ellipsoidal shapes (51). PS had a relatively high amylopectin content compared to other starches. Amylopectin is highly branched, which leads to a more open and less tightly packed structure within the granule. The branching

nature of amylopectin results in a less compact arrangement of starch molecules, contributing to the observed morphology of PS granules (52).

3.4. pH, Paste Clarity, and Freeze Thaw Stability

The pH, paste clarity, and thaw stability values of the starches are tabulated in Table 1. pH is a critical parameter that influences the functional properties and stability of various food ingredients, including starches. The pH values of the starches examined in this study are as follows: native starch from banana pseudostem (NSBP) (6.73 ± 0.04), resistant starch (type III) from banana pseudostem (RSBP) (6.84 ± 0.05), potato starch (PS) (6.43 ± 0.03), and corn starch (CS) (5.73 ± 0.06). These values indicate the relative acidity or alkalinity of the starch samples, with lower pH values indicating greater acidity (53). The pH value of NSBP indicates a slightly acidic to neutral nature. The pH of starch can be influenced by various factors, including the pH of the extraction medium, enzymatic activity, and the presence of organic acids within the sample (54). RSBP demonstrates a slightly higher pH value compared to NSBP. This increase in pH fro RSBP might be attributed to a specific structural property, such as increased amylose content or modified crystallinity, which can occur during autoclaving (55). Increased amylose content in corn starch generally enhances its resistance to pH variations. High-amylose corn starches form stronger gels and exhibit greater stability across different pH levels due to the robust network structure created by amylose molecules. This improved gel strength and stability result in reduced pH sensitivity, allowing the starch to maintains its texture and consistency better under acidic or basic conditions. Additionally, high-amylose starches show less swelling in acidic environments, further contributing to their stability (56).

Table 1. Paste clarity, pH, and freeze thaw stability of starches.

Parameter	Samples			
	NSBP	RSBP	PS	CS
pH	6.73 ± 0.04^{b}	6.84 ± 0.05^{a}	6.43 ± 0.03^{c}	5.73 ± 0.06^{d}
Paste Clarity (%)	14.77 ± 0.06^{c}	23. 7 ± 2.20^{b}	91.17 ± 0.06^{a}	5.73 ± 0.03^{d}
Thaw Stability (%)	4.00 ± 1.00^{d}	20.00 ± 0.58^{a}	14.33 ± 2.08^{b}	7.00 ± 1.00^{c}

Values represent the average of three repetitions ± standard deviation. Different letters in the same row are significantly different ($p < 0.05$).
NSBP: native starch of banana pseudostem, RSBP: resistant starch (type III) of banana pseudostem, PS: potato starch, CS: corn starch

In this study, PS exhibits a pH value of 6.43 ± 0.03, indicating a slightly acidic nature. The pH value of PS typically falls within the range of 6.0 to 7.0 (57). PS is widely utilized in the food industry due to its excellent water-binding capacity, viscosity, and textural properties. Reddy et al. (58) reported that the pH value of CS ranges from 5.0 to 7.0, which aligns well with the results obtained in this study. CS demonstrates the lowest pH value (5.73 ± 0.06) among the investigated starches. The pH of CS can be affected by factors such as corn variety, processing methods, and the presence of organic acids (54). CS is a versatile ingredient used in a wide range of food applications, including thickening, stabilizing, and texturizing, due to its unique properties (59). In industrial applications, higher paste clarity is generally more desirable, especially for products where visual appeal and transparency are important, such as sauces, gels, and certain food products. High paste clarity indicates a smoother and more uniform

starch gel, which is often preferred for its aesthetic quality and consistency (45). Conversely, lower paste clarity, which typically results from higher amylose content, may be acceptable in applications where opacity or a more robust gel structure is needed, such as in certain types of food or packaging materials (60). PS exhibits the highest clarity value with a mean value of 91.17% ± 0.06, followed by RSBP with a mean value of 23.7% ± 2.20, NSBP with a mean value of 14.77% ± 0.06 and CS with the lowest clarity value of 5.73% ± 0.06. According to Mehboob et al. (61), the higher the clarity value, the more transparent the starch appears. This indicates that PS presents a clearer visual appearance compared to the other samples. Clarity value is influenced by factors such as the amylose-amylopectin ratio, granule size, and the presence of impurities or other components in the starch (62). Kim et al. (52) explained that the high clarity value of PS can be attributed to its high amylopectin content, which contributes to its gelatinization properties and ability to form clear gels. In addition, the presence of a high content of phosphate monoesters rather than phospholipids typically found in cereal starches, mayalso contribute to the high paste clarity of PS (63). This characteristic makes PS desirable as a food additive in cooking various food, such as soups, sauces, and dressings without altering the color of the products. Therefore, understanding the clarity characteristics of different starches is crucial for selecting the appropriate starch for specific applications in the food and industrial sectors.

Furthermore, RSBP shows a relatively high clarity value compared to NSBP, indicating that the autoclaving process applied during the production of RSBP may have improved its clarity value. The presence of resistant starch in RSBP adds to its potential as a functional ingredient in food formulations, providing textural and sensory benefits (64). In contrast, NSBP exhibits a significantly ($p<0.05$) lower clarity value than both PS and RSBP. The lower clarity value of NSBP may be attributed to its composition, granule size, or the presence of impurities. CS demonstrated the lowest transparency among the evaluated starches. The low clarity value of CS could be attributed to its composition, physical properties, or processing techniques. CS typically has a higher amylose content compared to other starches, which may contribute to reduced translucency, leadinf to precipitate formation (65).

Freeze thawing refers to the process which water repeatedly freezes and thaws while in a frozen state. Freeze thawing serves as an indicator of quality in “ready-to-eat” and frozen products, as it impacts both texture and sensory perception (66). There was a significant ($p<0.05$) difference among all the examined starches, with RSBP showing the highest percentage of thaw stability. This was attributed to the RSBP having undergone retrogradation, which enhances the gel formation properties of resistant starch and helps reduce syneresis. Resistant starches often have a more stable gel network due to their ability to retain water better and resist breakdown during freeze-thaw cycles (67). This makes them more suitable for products requiring better textural stability after freezing.

PS granules tend to be larger and more irregularly shaped compared to other starches. Larger granules with irregular shapes can result in a less compact gel structure and increased syneresis (68). Furthermore, CS showed a significantly lower thaw stability (7.00 ± 1.00) than RSBP and PS, indicating a moderate ability to resist syneresis. The higher amylose content in corn starch compared to NSBP and PS contributes to its relatively better stability. CS forms more cohesive gel networks that can better retain water during freeze-thaw cycles, though it still exhibits some degree of syneresis. Therefore, the present results are in good agreement with those presented in Figure 3. Moreover, NSBP had the lowest percentage of thaw stability

value (4.00 ± 1.00), indicating that the starch granules require a higher temperature to fully absorb water and swell, forming a stable gel structure (68).

3.5. Particle Size Distribution

The results of particle size distribution of the starches are shown in Table 2. D (0.5) refers to the median diameter of the particle size distribution, representing the particle diameter at which 50% of the particles are smaller and 50% are larger in the cumulative distribution (69). There was no significant ($p>0.05$) difference between NSBP and RSBP for particle size distribution, which ranged from 20.73 ± 0.78 in RSBP to 22.77 ± 2.77 in NSBP. This indicates that 50% of the particles in NSBP and RSBP are respectively larger than 22.77 µm and 20.73 µm, while 50% are smaller than these values. Moreover, the results also indicate that the autoclave treatment did not affect to the particle size distribution of the starches. Compared to other starch sources, the pseudostem starch granules are often smaller and more evenly distributed. The inherent quality of pseudostem helps minimize the particle size distribution. RSBP and NSBP, both obtained from banana pseudostem, underwent a refining process to remove contaminants and undesirable elements. Washing and filtration was repeated many times to eliminate extraneous materials during the refining process. These processes contribute to a lower particle size distribution by reducing the size of the particles (70).

Table 2. Particle size distribution of starches.

Sample	D(0.5)/µm
NSBP	22.77 ± 2.77[b]
RSBP	20.73 ± 0.78[b]
PS	45.22 ± 2.63a
CS	15.53 ± 0.93c

Values represent the average of three repetitions ± standard deviation. Different letters in a column are significantly different ($p < 0.05$).
D (50): mean diameter of starch granules when the cumulative distribution of particles diameter is 50%.
NSBP: native starch of banana pseudostem, RSBP: resistant starch (type III) of banana pseudostem, PS: potato starch, CS: corn starch

There was a significantly ($p<0.05$) higher mean value of particle size distribution (45.22 ± 2.63) in PS compared to the other samples. The value of d (0.5) = 35.03 µm indicates the median particle size of PS. PS presented the highest particle size value because its granules have a unique structure characterized by a large central hilum (or pore) and irregular shapes. This structure affects the overall particle size of PS, with the presence of the hilum and the irregular shape contributing to the larger average particle size. The mean value of PS was also consistent with data presented by Domene-López et al. (71), which reported a mean value (µm) of 46.02 ± 0.05. On the other hand, CS showed a significantly ($p<0.05$) lowest mean value of particle size distribution (15.53 ± 0.93). This was associated with the morphology of corn starch granules, which have a more uniform and spherical shape compared to other starch sources. Granules of corn starch are generally smaller (Figure 3) and more tightly packed, contributing to a smaller particle size distribution. According to Lv et al. (69), starch granule with a particle size smaller than 2.72 µm are classified small, those ranging from 2.27 to 17.51

µm are considered medium, and granules larger than 17.51 µm are defined as large. Therefore, based on the size classification by Lv et al. (69), it can be concluded that NSBP, RSBP, and PS have large starch granules, while CS has medium starch granules.

4. Conclusions

Resistant starch (type III) processed from banana pseudostem through an autoclaving process, was confirmed via the functional groups detected in Fourier-transform infrared spectroscopy. The presence of sulphate group in resistant starch (type III) indicates that the starch is more resistant to enzymatic breakdown. Moreover, starches from banana pseudostem (i.e., native and resistant starch (type III)) were found to have a similar B-type crystalline structure to that of commercial potato starch. All evaluated starches showed a slightly acidic to neutral nature (pH 5.73-pH 6.84). The autoclaving process during the production of resistant starch (type III) improved paste clarity without affecting the particle size distribution of native banana pseudostem starch. However, this process caused detrimental effect on the native starch of banana pseudostem, resulting in a higher thaw stability value and destruction of the native arrangement of the starch granules. Banana pseudostem can be considered a feasible raw material for obtaining low-cost native starch as well as resistant starch (type III) for use in various food products, such as confectionery, bakery items, sauce, and syrups. These findings not only help reduce waste from banana cultivation but also pave the way for developing innovative, health-oriented food products, thereby supporting sustainable practices and enhancing nutritional options.

Acknowledgements

We thank Mr. Syahril Amin bin Hashim from the Centralized Lab Management Centre, UniSZA for technical support in operating the Field Emission Scanning Electron Microscope. We extend our gratitude to the Ministry of Education Malaysia for financial support.

Author Contributions

F L.H.H: Methodology, supervision, conceptualization, coordinator, validation data, and writing (review and editing); R.S. and F.S.M.: Conduct analysis, data analysis, writing the original draft; S.H.Z. and S.A.H.T.M.: Conduct analysis and review the manuscript.

Funding

The study was funded by the Ministry of Education Malaysia under the Project Fundamental Research Grant Scheme for Research Acculturation of Early Career Researchers (RACER) 2019 grant (RACER/1/2019/TK02/UNISZA//1; RR292).

Institutional Review Board Statement

Not applicable.

Data Availability Statement

The data supporting the findings of the article is available within the article.

Conflicts of Interest

All authors declare there is no conflict of interest, financial or otherwise in this research.

References

1. Subagyo A, Chafidz A. Banana pseudo-stem fiber: preparation, characteristics, and applications. In *Banana Nutrition – Function and Processing Kinetics*. Jideani AIO, Anyasi TA. (Eds.) [Internet]. London (UK): IntechOpen; 2020:1-19. Available from: http://dx.doi.org/10.5772/intechopen.82204
2. Tan BC. Can banana be a success story for Malaysia? J. Agribus. Mark. [Internet]. 2022;9(1):13–22. Available from: https://doi.org/10.56527/jabm.9.1.2
3. FAO (Food and Agriculture Organization of the United Nations). FAOSTAT: Production Indices. [Internet]. 2024. Available from: https://www.fao.org/faostat/en/#data/QCL
4. Silva FS, Ribeiro CEG, Demartini TJDC, Rodríguez RJS. Physical, chemical, mechanical, and microstructural characterization of banana pseudostem fibers from *Musa Sapientum*. Macromol. Symp. [Internet]. 2020;394:2000052. Available from: https://doi.org/10.1002/masy.202000052
5. Makroo HA, Naqash S, Saxena J, Sharma S, Majid D, Dar BN. Recovery and characteristics of starches from unconventional sources and their potential applications: A review. Appl. Food Res. [Internet]. 2021;1(1):100001. Available from: https://doi.org/10.1016/j.afres.2021.100001
6. Apriyanta A, Compart J, Fettke J. A review of starch, a unique biopolymer – Structure, metabolism and in planta modifications. Plant Sci. [Internet]. 2022;318:111223. Available from: https://doi.org/10.1016/j.plantsci.2022.111223
7. Luo M, Gong W, Zhang S, Xie L, Shi Y, Wu D, Shu X. Discrepancies in resistant starch and starch physicochemical properties between rice mutants similar in high amylose content. Front. Plant Sci. [Internet]. 2023;14:1267281. Available from: https://doi.org/10.3389%2Ffpls.2023.1267281
8. Englyst HN, Veenstra J, Hudson GJ. Measurement of rapidly available glucose (RAG) in plant foods: a potential in vitro predictor of the glycaemic response. Br. J. Nutr. [Internet]. 1996;75:327–337. Available from: https://doi.org/10.1079/bjn19960137
9. Bojarczuk A, Skąpska S, Khaneghah AM, Marszałek K. Health benefits of resistant starch: A review of the literature. J. Funct, Foods. [Internet]. 2022;93:105094. Available from: https://doi.org/10.1016/j.jff.2022.105094
10. Wang Z, Wang S, Xu Q, Kong Q, Li F, Lu L, Xu Y, Wei Y. Synthesis and functions of resistant starch. Adv. Nutr. [Internet]. 2023;14(5):1131–1144.
11. Apriyanto A, Compart J, Fettke J. A review of starch, a unique biopolymer – structure, metabolism and in planta modifications. Plant Sci. [Internet]. 2022;318:111223. Available from: https://doi.org/10.1016/j.plantsci.2022.111223
12. Englyst HN, Kingman SM. Cummings JH. Classification and measurement of nutritionally important starch fractions. Eur. J. Clin. Nutr. [Internet]. 1992;46(Suppl2):S33–50. Available from: https://www.researchgate.net/publication/21824238_Classification_and_Measurement_of_Nutritionally_Important_Starch_Fractions
13. Wen J-J, Li M-Z, Hu J-L, Tan H-Z, Nie S-P. Resistant starches and gut microbiota. Food Chem. [Internet]. 2022; 387:132895. Available from: https://doi.org/10.1016/j.foodchem.2022.132895
14. Klostermann C, Endika MF, Kouzounis D, Buwalda PL, de Vos P, Zoetendal EG, Bitter JH, Schols HA. Presence of digestible starch impacts in vitro fermentation of resistant starch. Food Funct. [Internet]. 2024;15:223–235. Available from:

https://doi.org/10.1039/D3FO01763J
15. DeMartion P, Cockburn DW. Resistant starch: Impact on the gut microbiome and health. Curr Opin Biotechnol. [Internet]. 2020;61:66–71.
16. Dobranowski PA, Stintzi A. Resistant starch, microbiome, and precision modulation. Gut Microbes. [Internet]. 2021;13(1):1926842. Available from: https://doi.org/10.1080%2F19490976.2021.1926842
17. Kim MK, Park J, Kim D-M. Resistant starch and type 2 diabetes mellitus: Clinical perspective. J. Diabetes Investig. [Internet]. 2024;15(4):395–401. Available from: https://doi.org/10.1111%2Fjdi.14139
18. Xiong K, Wang J, Kang T, Xu F, Ma A. Effects of resistant starch on glycaemic control: A systematic review and meta-analysis. Br. J. Nutri. [Internet]. 2021;125:1260–1269. Available from: https://doi.org/10.1017/S0007114520003700
19. Maëliss C, Anne-Laure C, Sophie V, Julie-Anne N. The impact of slowly digestible and resistant starch on glucose homeostasis and insulin resistance. Crr. Opin. Clin. Nutr. Metab. Care. [Internet]. 2024;27(4):338–343. Available from: https://doi.org/10.1097/MCO.0000000000001044
20. Rashed AA, Saparuddin F, Rathi D-NG, Nasir NNM, Lokman EF. Effects of resistant starch interventions on metabolic biomarkers in pre-diabetes and diabetes adults. Front. Nutr. [Internet]. 2022;8:793414. Available from: https://doi.org/10.3389/fnut.2021.793414
21. Tekin T, Fisunoglu M. A comprehensive review resistant starch-containing bread as a functional food: Its effect on appetite, glycemic index, and glycemic response. Starch. [Internet]. 2023;75(9-10):2200291. Available from: https://doi.org/10.1002/star.202200291
22. Karunarathna S, Wickramasinghe I, Truong T, Brennan C, Navaratne SB, Chandrapala J. Development of low-calorie food products with resistant starch-rich sources. – A review. Food Rev. Int. [Internet]. 2023;40(2):814–831. Available from: https://doi.org/10.1080/87559129.2023.2204137
23. Walsh SK, Lucey A, Walter J, Zannini E, Arendt EK. Resistant starch – An accessible fiber ingredient acceptable to the Western palate. Compr. Rev. Food Sci. Food Saf. [Internet]. 2022;21(3):2930–2955. Available from: https://doi.org/10.1111/1541-4337.12955
24. Pillai GS, Morya S, Khalid W, Khalid MZ, Almalki R, Siddeeg A. Banana pseudostem: An undiscovered fiber enriched sustainable functional food. J. Nat. Fibers. [Internet]. 2024;21(1):2304004. Available from: https://doi.org/10.1080/15440478.2024.2304004
25. Nakthong N, Wongsagonsup R. Amornsakchai T. Characteristics and potential utilizations of starch from pineapple stem waste. Ind. Crops Prod. [Internet]. 2017;105: 74–82. Available from: https://doi.org/10.1016/j.indcrop.2017.04.048
26. Rahma A, Adriani M, Rahayu P, Tjandrawinata RR, Rachmawati H. Green isolation and physical modification of pineapple stem waste starch as pharmaceutical excipient. Drug Dev. Ind. Pharm. [Internet]. 2019;45(6):1029–1037. Available from: https://doi.org/10.1080/03639045.2019.1593438
27. Zi-Ni T, Rosma A, Karim AA, Liong MT. Functional properties of resistant starch type-III from *Metroxylon sagu* as affected by processing conditions. Pertanika J. Trop. Agric. Sci. 2015;38(3):399–412.
28. Rashid ZM, Mohd-Nasir NN, Wan-Ahmad WN, Mahmod NH. α- glucosidase inhibition, DPPH scavenging and chemical analysis of polysaccharide extracts of *Aquilaria* sp. leaves. J. Agrobiotechnol. [Internet]. 2020;11(2):59–69. Available from:

https://doi.org/10.37231/jab.2020.11.2.225
29. Lian X, Cheng K, Wang D, Zhu W, Wang X. Analysis of crystals of retrograded starch with sharp X-ray diffraction peaks made by recrystallization of amylose and amylopectin. Int. J. Food Prop. [Internet]. 2017;20(Sup3):S3224–S3236. Available from: https://doi.org/10.1080/10942912.2017.1362433
30. Aoyagi T, Oshima T, Imaizumi T. Quantitative characterization of individual starch grain morphology using a particle flow analyzer. LWT. [Internet]. 2021;139:110589. Available from: https://doi.org/10.1016/j.lwt.2020.110589
31. Das A, Sit N. Modification of taro starch and starch nanoparticles by various physical methods and their characterization. Starch-Stärke. [Internet]. 2021;73(5-6):2000227. Available from: https://doi.org/10.1002/star.202000227
32. Vijayakumar, PP, Adedeji A. Measuring the pH of food products. University of Kentucky;2017. Available from: https://www.researchgate.net/publication/330601448_Measuring_the_pH_of_Food_Products
33. Liu Y, Gao J, Feng D, Zhao J, Guo Y, Zhao J, Li W, Yan W. Modification of structural and physicochemical properties of repeated freeze-thawed cycle maize starch. Int. J. Food Prop. [Internet]. 2020;23(1):1597-1610. Available from: https://doi.org/10.1080/10942912.2020.1817070
34. Tao H, Wang P, Wu F, Jin Z, Xu X. Particle size distribution of wheat starch granules in relation to baking properties of frozen dough. Carbohydr Polym. [Internet]. 2016;137:147-153. Available from: https://doi.org/10.1016/j.carbpol.2015.10.063
35. Aziz N, Zin BM, Rashid ZM. Antioxidant and ATR-FTIR-based chemometric of wild Erechtites species leaves extracts. Biosci. Res. [Internet]. 2022;19(SI-1):6372. Available from: http://www.isisn.org/BR-19-SI-1-2022/63-72-7-BR-SI-FBIM-2022-ZALILAWATI.pdf
36. Espinosa-Solis V, Zamudio-Flores PB, Espino-Díaz M, Vela-Gutiérrez G, Rendón-Villalobos JR, Hernández-González M, Hernández-Centeno F, Peña HYLDL, Salgado-Delgodo R, Ortega-Ortega A. Physicochemical characterization of resistant starch type-III (RS3) obtained by autoclaving Malanga (*Xanthosoma sagittifolium*) flour and corn starch. Molecules. [Internet]. 2021;26(13):1-13. Available from: https://doi.org/10.3390/molecules26134006
37. Pourmohammadi K, Abedi E. The effect of pre and post-ultrasonication on the aggregation structure and physicochemical characteristics of tapioca starch containing sucrose, isomalt and maltodextrin. Int. J. Biol. Macromol. [Internet]. 2020;163:485–496. Available from: https://doi.org/10.1016/j.ijbiomac.2020.06.205
38. Dankar I, Haddarah A, Omar FEL, Pujolà M, Sepulcre F. Characterization of food additive-potato starch complexes by FTIR and X-ray diffraction. Food Chem. [Internet]. 2018;260:7–12. Available from: https://doi.org/10.1016/j.foodchem.2018.03.138
39. Singh R, Sharanagat VS. Physico-functional and structural characterization of ultrasonic-assisted chemically modified elephant foot yam starch. Int. J. Biol. Macromol. [Internet]. 2020;164:1061–1069. Available from: https://doi.org/10.1016/j.ijbiomac.2020.07.185
40. Rodriguez pineda LM, Muñoz-Prieto Ede, Rius-Alonso CA, Palacios-Alquisira J. Preparation and characterization of potato starch nanoparticles with acrylamide by microwave radiation. Cienc. Desarro. [Internet]. 2018;9(2):149–159. Available from: https://doi.org/10.19053/01217488.v9.n2.2018.7783
41. Torrenegra M, Solano R, Herrera A, Len G, Pajaro A. Fourier transform infrared

spectroscopy (FTIR) analysis of biodegradable films based on modified Colombian starches of cassava and yam. Int. J. Chemtech Res. [Internet]. 2018;11(11): 184–192. Available from: https://doi.org/10.20902/ijctr.2018.111118

42. Ibrahim N, Zakaria AJ, Ismail Z, Ahamad Y, Mohd KS. Application of GCMS and FTIR fingerprinting in discriminating two species of Malaysian stingless bees propolis. Int. J. Eng. Technol. [Internet]. 2018;7(4.43):106-112. Available from: https://www.researchgate.net/publication/334284691_Application_of_GCMS_and_FTIR_Fingerprinting_in_Discriminating_Two_Species_of_Malaysian_Stingless_Bees_Propolis
43. Samir A, Ashour FH, Hakim AAA, Bassyouni M. Recent advances in biodegradable polymers for sustainable applications. Mater. Degrad. [Internet]. 2022;6(68):321. Available from: https://doi.org/10.1038/s41529-022-00277-7
44. Dong H, Vasanthan T. Effect of phosphorylation techniques on stractural, thermal, and pasting properties of pulse starches in comparision with corn starch. Food Hydrocoll. [Internet]. 2020;109:106078. Available from: https://doi.org/10.1016/j.foodhyd.2020.106078
45. Yan X, McClements DJ, Luo S, Liu C, Ye J. Recent advances in the impact of gelatinization degree on starch: Structure, properties and applications. Carbohydr. Polym. [Internet]. 2024;340:122273. Available from: https://doi.org/10.1016/j.carbpol.2024.122273
46. Luchese CL, Spada JC, Tessaro IC. Starch content affects physicochemical properties of corn and cassava starch-based films. Ind. Crops Prod. [Internet]. 2017;109:619–626. Available from: https://doi.org/10.1016/j.indcrop.2017.09.020
47. Dome K, Podgorbunskikh E, Bychkov A, Lomovsky O. Changes in the crystallinity degree of starch having different types of crystal structure after mechanical pretreatment. Polymers. [Internet]. 2020;12(3): 641. Available from: https://doi.org/10.3390%2Fpolym12030641
48. Rodriguez-Garcia ME, Hernandez-Landaverde MA, Delgado JM, Ramirez-Gutierrez CF, Ramirez-Cardona M, Millan-Malo BM, Londoño-Restrepo SM. Crystalline structures of the main components of starch. Curr. Opin. Food Sci. [Internet]. 2021;37:107–111. Available from: https://doi.org/10.1016/j.cofs.2020.10.002
49. Utrilla-Coello RG, Rodríguez-Huezo, ME, Carrillo-Navas H, Hernández Jaimes C, Vernon-Carter EJ, Alvarez-Ramirez J. *In vitro* digestibility, physicochemical, thermal and rheological properties of banana starches. Carbohydr. Polym. [Internet]. 2014;101:154-162. Available from: https://doi.org/10.1016/j.carbpol.2013.09.019
50. Marta H, Cahyana Y, Djali M. Pramafisi G. The properties, modification, and application of Banana Starch. Polymers [Internet]. 2022;14(15):3092. Available from: https://doi.org/10.3390/polym14153092
51. Tong C, Ma Z, Chen H, Gao H. Toward an understanding of potato starch structure, function, biosynthesis, and applications. Food Front. [Internet]. 2023;1-21. Available from: https://doi.org/10.1002/fft2.223
52. Kim HR, Choi SJ, Choi H-D, Park C-S, Moon TW. Amylosucrase- modified waxy potato starches recrystallized with amylose: The role of amylopectin chain length in formation of low-digestible fractions. Food Chem. [Internet]. 2020;318:126490. Available from: https://doi.org/10.1016/j.foodchem.2020.126490
53. Chatpapamon C, Wandee Y, Uttapap D, Puttanlek C, Rungsardthong V. Pasting properties of cassava starch modified by heat-moisture treatment under acidic and alkaline pH

environments. Carbohydr. Polym. [Internet]. 2019;215:338–347. Available from: https://doi.org/10.1016/j.carbpol.2019.03.089
54. Mazareli RCdS, Montoya ACV, Delforno TP, Centurion VB, Oliveira VMd, Silva EL, Varesche MBA. Enzymatic routes to hydrogen and organic acids production from banana waste fermentation by autochthonous bacteria: optimization of pH and temperature. Int. J. Hydrog. Energy. [Internet]. 2021;46(12):8454-8468. Available from: https://doi.org/10.1016/j.ijhydene.2020.12.063
55. Duyen TTM, Huong NTM, Phi NTL, Hung PV. Physicochemical properties and *in vitro* digestibility of mung-bean starches varying amylose contents under citric acid and hydrothermal treatments. Int. J. Biol. Macromol. [Internet]. 2020;164:651-658. Available from: https://doi.org/10.1016/j.ijbiomac.2020.07.187
56. Obedi M, Qi Y, Xu B. High-amylose maize starch: Strucutre, properties, modifications and industrial applications. Carbohydr Polym. [Internet]. 2023;299:120185. Available from: https://doi.org/10.1016/j.carbpol.2022.120185
57. Singh MP, Kanawjia SK, Giri A, Khetra Y. Effect of potato starch on quality characteristics of shredded mozzarella cheese during storage. J. Food Sci. Technol. [Internet]. 2015;52(11):7507–7512. Available from: https://doi.org/10.1007/s13197-015-1807-2
58. Reddy CK, Pramila S, Haripriya S. Pasting, textural and thermal properties of resistant starch prepared from potato (S*olanum tuberosum*) starch using pullulanase enzyme. J. Food Sci. Technol. [Internet]. 2013;5*2*(3):1594– 1601. Available from: https://doi.org/10.1007/s13197-013-1151-3
59. Ketthaisong D, Suriharn B, Tangwongchai R, Jane J, Lertrat K. Physicochemical and morphological properties of starch from fresh waxy corn kernels. J. Food Sci. Technol. [Internet]. 2015;52(10):6529–6537. Available from: https://doi.org/10.1007/s13197-015-1750-2
60. Zhong Y, Tai L, Blennow A, Ding L, Herburger K, Qu J, Xin Z, Guo D, Hebelstrup KH, Liu X. High-amylose starch: Structure, functionality and applications. Crit. Rev. Fod Sci. Nutr. [Internet]. 2023;63(27): 8568-8590. Available from: https://doi.org/10.1080/10408398.2022.2056871
61. Mehboob S, Ali TM, Sheikh M, Hasnain A. Effects of cross linking and/or acetylation on sorghum starch and film characteristics. Int. J. Biol. Macromol. [Internet]. 2020;155, 786–794. Available from: https://doi.org/10.1016/j.ijbiomac.2020.03.144
62. Yu Z, Wang Y-S, Chen H-H, Li Q-Q. Effect of sodium alginate on the gelatinization and retrogradation properties of two tuber starches. Cereal Chem. [Internet] 2018;95(3):445–455. Available from: https://doi.org/10.1002/cche.10046
63. Arueya GL, Ojesanmi AA. Evaluation of effects of increasing molar substitution of hydroxypropylene on physicochemical, functional and morphological properties of starch from water yam (*Dioscorea alata*). J. Food Res. [Internet]. 2019;8(4), 58-88. Available from: https://doi.org/10.4172/2472-0542-C1-009
64. Kumar R, Khatkar B.S. Thermal, pasting and morphological properties of starch granules of wheat (*T*riticum *aestivum* L.) varieties. J. Food sci. Technol. [Internet]. 2017;54(8):2403-2410. Available from: https://doi.org/10.1007%2Fs13197-017-2681-x
65. Lutfi Z, Kalim Q, Shahid A, Nawab A. Water chestnut, rice, corn starches and sodium alginate. A comparative study on the physicochemical, thermal and morphological characteristics of starches after dry heating. Int. J. Biol. Macromol. [Internet]. 2021;184:476–482. Available from: https://doi.org/10.1016/j.ijbiomac.2021.06.128

66. Chen Y-F, Kaur L, Singh J. Chemical modification of starch. In *Starch In Food Structure, Function and Applications.* Sjöö M, Nilsson L. (Eds.) [Internet]. Cambridge(UK): Woodhead Publishing; 2018: 283–321. Available from: https://doi.org/10.1016/b978-0-08-100868-3.00007-x
67. Srichuwong S, Isono N, Jiang H, Mishima T, Hisamatsu M. Freez-thaw stability of starches from different botanical sources: Correlation with structural features. Carbohydr Polym. [Internet]. 2012;87(2):1275-1279. Available from: https://doi.org/10.1016/j.carbpol.2011.09.004
68. Ghalambor P, Asadi G, Nafchi AM, Ardebili SMS. Investigation of dual modification on physicochemical, morphological, thermal, pasting, and retrogradation characteristics of sago starch. Food Sci. Nutr. [Internet]. 2022;10(7):2285-2299.
69. Lv Z, Yu K, Jin S, Ke W, Fei C, Cui P, Lu G. Starch granules size distribution of sweet potato and their relationship with quality of dried and fried produces. Starch-Stärke. [Internet]. 2019;71(5-6):1800175. Available from: https://doi.org/10.1002/star.201800175
70. Sarkar A, Fum BX. Impact of quality improvement and milling innovations on durum wheat and end products. Foods. [Internet]. 2022;11(12):1796. Available from: https://doi.org/10.3390/foods11121796
71. Domene-López D, Garcia-Quesada JC, Martin-Gullon I, Montalbán MG. Influence of starch composition and molecular weight on physicochemical properties of biodegradable films. Polymers [Internet]. 2019;11(7):1084. Available from: https://doi.org/10.3390/polym11071084